Structural Isomerization and Molecular Motions of Liquid *n*-Alkanes. Ultrasonic and High-Frequency Shear Viscosity Relaxation

R. Behrends and U. Kaatze*

Drittes Physikalisches Institut, Universität Göttingen, Bürgerstrasse 42-44, D-37073 Göttingen, Germany

Received: November 12, 1999; In Final Form: February 7, 2000

Between 20 and 120 MHz, the complex shear viscosity of *n*-tetradecane, *n*-pentadecane, *n*-hexadecane, and a *n*-eicosane/*n*-tetradecane mixture has been measured using a shear impedance spectrometer. The data are compared to ultrasonic absorption spectra of the liquids as measured between 1 MHz and 2 GHz. Relaxational behavior has been found. The extrapolated high-frequency shear viscosity $\eta_s(\infty)$ is distinctly smaller than the static shear viscosity $\eta_s(0)$. The shear viscosity relaxation time is discussed in light of literature data of the orientational correlation time from depolarized Rayleigh scattering and also of the collision time as resulting from dielectric spectrometry. The assumption appears to be likely that the shear viscosity relaxation is due to rotational isomerizations of the chain molecules. A damped torsional oscillator model has been used to evaluate the spectra. The reasonable number of three carbon atoms per oscillator unit results. The activation energies and enthalpies are derived from measurements at different temperatures.

1. Introduction

The shear viscosity η_s of liquids reflects in an obvious manner the intermolecular forces that are responsible not only for the existence of condensed matter at all but also for specific differences in the properties of condensed fluids. Despite the fundamental importance of intermolecular forces to the study of liquids and regardless of the key position of the shear viscosity in a great variety of transport phenomena in fluids,[1] comparatively little is known on the frequency-dependent behavior of η_s in low-viscosity liquids. Since the knowledge of relaxational characteristics in the shear viscosity may provide valuable insights into the molecular interactions of liquids, allowing one to set up models of elementary processes that take place in the molecules, we have studied experimentally the frequency-dependent (complex) shear viscosity of the liquid *n*-alkanes using a shear impedance spectrometric method. We combined these measurements with broad-band ultrasonic spectrometry of the liquids. Alkanes have been studied here in order to first exclude effects from association due to hydrogen bonding. Additional interest springs from conflicting models of the viscoelastic properties of liquid *n*-alkanes.[2,3]

2. Experimental Section

Sample Liquids. A previous study of the ultrasonic absorption spectra of *n*-decane, *n*-dodecane, *n*-tetradecane, and *n*-hexadecane at 25 °C clearly revealed relaxation behavior.[4] The relaxation frequency ν_r of the relaxation process with discrete relaxation time $\tau = (2\pi\nu_r)^{-1}$ increased with increasing length of the hydrocarbon molecule. For decane ν_r just coincides with the upper limit (2 GHz) of our present measuring range. We thus focused on longer normal alkanes $CH_3(CH_2)_{n-2}CH_3$, $n \geq 14$, here. We used *n*-tetradecane ($n = 14$, Fluka, >99%), *n*-pentadecane ($n = 15$, Fluka, >99.8%, Sigma, >99%), *n*-hexadecane ($n = 16$, Fluka, >98%), and *n*-eicosane ($n = 20$, Fluka, >97%). Because *n*-eicosane is a solid at room temperature (melting point: 36 °C), we measured an eicosane/tetradecane mixture with mole fraction $x = 0.33$ of the higher homologue. To also study the effect of dilution, *n*-pentadecane/*n*-hexane mixtures with mole fraction $x = 0.75$ and $x = 0.5$ of pentadecane have been included. Since *n*-hexane ($n = 6$; Fluka, >99.5%) did not show any relaxation characteristics in the measuring frequency range, it may be taken as an ideal (inert) solvent. The solutions were prepared by weighing appropriate amounts of the constituents into suitable flasks.

The density ρ of the sample liquids has been determined picnometrically. The *static* shear viscosity $\eta_{s0} = \eta_s$ ($\nu \rightarrow 0$) has been measured using a falling ball viscometer (Haake, B/BH) and also a set of Ubbelohde-type capillary viscometers (Schott, KPG). The η_{s0} values given in Table 1 are weighted means of the data measured with both methods.

Ultrasonic Absorption Spectrometry. We have used two parallel experimental approaches to investigate the shear viscosity relaxation of alkanes. One utilizes longitudinal compressional (acoustic) waves. It is based on the dependence of the sonic absorption coefficient α upon the shear viscosity. For nonmetallic liquids, for which a small contribution from the heat conductivity can be neglected[5]

$$\alpha = \frac{8\pi\nu^2}{3\rho c^3}\left(\eta_s + \frac{3}{4}\eta_v\right) \tag{1}$$

where ν denotes the frequency of measurement and c the sound velocity of the liquid. The volume viscosity η_v is related to the curl-free part of the acoustic field. If no high-frequency relaxation processes contribute to the volume viscosity, $\eta_v = 2/3\ \eta_s$ is found.[6] Hence a minimum sonic absorption coefficient

$$\alpha_{min} = \frac{4\pi\nu^2}{\rho c^3}\eta_s \tag{2}$$

is expected to exist in fluids. In deriving eq 1 it is tacitly assumed that no other relaxation mechanisms contribute to the absorption coefficient within the frequency range under consideration.

10.1021/jp994015z CCC: $19.00
Published on Web 03/24/2000

TABLE 1: Survey of the Sample Liquids as Well as Density (ρ) and Static Shear Viscosity (η_{s0}) Data at Some Temperatures T[a]

sample	T, °C	ρ, mg/cm^3	η_{s0}, mPa·s
n-tetradecane	25.0	760.0	2.05
	18.5	764.0	
	10.0	766.0	
n-pentadecane	25.0	764.0	2.55
	20.0	769.0	
	15.0	771.0	3.20
n-pentadecane/*n*-hexane, $x = 0.75$	15.0	759.3	2.19
n-pentadecane/*n*-hexane, $x = 0.5$	15.0	738.5	1.31
n-hexadecane	25.0	770.0	3.05
	20.0	773.0	
	18.5	774.0	
n-eicosane/*n*-tetradecane ($x = 0.333$)	25.0	769.4	3.13

[a] The mole fraction x refers to the higher homologue in a mixture.

We applied two methods to measure the absorption coefficient α of the liquids in the frequency range from 1 MHz to 2 GHz. At low frequencies, where α is small, we used a plano-concave[7] and a biplanar[8] cavity resonator cell for fixed path-length continuous wave measurements of the quality factor relative to a carefully chosen reference liquid. At $\nu > 20$ MHz three specimen cells were utilized for the direct determination of α by a variable path-length pulse-modulated wave transmission technique. The cells mainly differed in the parameters of the transducers (30 MHz $\leq \nu <$ 500 MHz: lithium niobate disks, transducer diameter $2R_T = 12$ mm, fundamental frequency of thickness vibrations $\nu_T = 10.8$ MHz, overtone operation at $\nu = (2n+1)\,\nu_T$, $n = 1, 2, ...$;[9] 500 MHz $\leq \nu <$ 2 GHz: broad-band end face excitation[10] of lithium niobate rods, $2R_T = 3$ mm, length $l_T = 10$ mm;[11,12] 1.3 GHz $\leq \nu <$ 4.6 GHz: zinc oxide layers sputtered on circular delay lines made of sapphire with diameter $2R_T = 7$ mm, $\nu_T = 1.3$ GHz, overtone operation).[12]

The temperature of all specimen cells was controlled to within ±0.05 K, and it was measured with an accuracy of ±0.02 K. Temperature differences between the different cells were thus smaller than ±0.05 K, resulting in an estimated error of less than 0.1% in the values of the absorption coefficient α. At all frequencies highly stable synthesized signal generators have been used. Hence frequency fluctuations can be neglected throughout.

With the resonator measurements, the main sources of possible errors are small disturbances in the cell geometry, in particular, small deformations occurring during the emptying, cleaning, and refilling procedure when the sample is exchanged for the reference. Repeated filling of the cavity cells resulted in an estimated uncertainty of about 5% in the α value, including also the error that might result from small deviations of the sound velocity and the density of the reference liquid from the respective sample data. A significantly higher accuracy ($\Delta\alpha/\alpha \approx 1\%$) has been achieved in the pulse-modulated traveling wave transmission measurements since this method does not need a reference liquid. At higher frequencies, depending on the absorption coefficient of the liquid, the usable sample thickness range in the measurements may be so small that the limited accuracy of the distance meter (±5 nm with the cell that uses ZnO films as transducers, ±200 nm otherwise) cannot be neglected.

Shear Impedance Spectrometry. The other approach is based on the determination of the complex shear wave impedance Z_s of the liquid as a function of frequency ν. To achieve a high sensitivity, sufficient for the study of low-viscosity liquids, we applied a shear resonator technique,[13] basically a further development of the method by Eggers and Funck.[14] The essential device of the setup was a disk-shaped AT-cut quartz ($2R_T = 15$ mm, thickness $d_T = 0.83$ mm) suitable for thickness shear oscillations. One end face of the disk was loaded with a thin layer ($d_L \approx 3$ mm) of the liquid under test. The resonator was operated at the odd harmonics of the AT-cut quartz fundamental frequency $\nu_{T,sh} = 2$ MHz. We got quality factors sufficiently high for reliable measurements ($Q \geq 80\,000$) in the frequency range between 20 and 120 MHz.

To precisely determine the resonance frequency $\nu_{r,n} = (2n + 1)\nu_{T,sh}$, $n = 1, 2, ...$, and quality factor $Q(\nu_{r,n})$ of each resonance peak, we always recorded the electrical cell impedance in a sufficiently broad frequency range around $\nu_{r,n}$, allowing for a careful consideration of higher order vibration modes.[13] The electrical impedance of the AT-quartz resonator was measured in a RF-bridge, enabling us to sensitively compensate for the high capacity of the device as resulting from the gold-coated transducer faces. The measured $\nu_{r,n}$ and $Q(\nu_{r,n})$ data yield the real part Z_s' and the imaginary part Z_s'' of the complex shear impedance $Z_s(\nu) = Z_s'(\nu) + iZ_s''(\nu)$,[15,16] from which the complex shear viscosity follows as

$$\eta_s(\nu) = \eta_s' - i\eta_s''(\nu) = \frac{(Z_s'(\nu) + iZ_s''(\nu))^2}{i\omega\rho} \qquad (3)$$

Herein $\omega = 2\pi\nu$ is the angular frequency. Measurements of reference liquids with well-known (static) viscosity η_{s0}, for which at frequencies up to 120 MHz no relaxation phenomena are expected, yielded the following experimental errors $\Delta\eta_s'/\eta_s'$: 0.05, 20 MHz $\leq \nu <$ 60 MHz; 0.03, 60 MHz $\leq \nu <$ 80 MHz; 0.1, 80 MHz $\leq \nu <$ 120 MHz.

Sound Velocity Measurements. The sound velocity c of the samples has been determined in connection with the measurements of the ultrasonic absorption coefficient. In the lower part of the frequency range of the measurements c has been derived from the distances between series of resonance frequencies of the cavity resonator cells, taking into account the nonequidistancy of the cell resonances due to incomplete reflection of the sonic waves at liquid/transducer interfaces.[7,17] At higher frequencies c was derived from the waviness in the transfer function of the variable path-length cells due to multiple reflections of the sonic signal at small transducer spacing. The experimental error in the sound velocity is $\Delta c/c = 0.001$ at $\nu <$ 3 MHz and $\nu >$ 500 MHz and $\Delta c/c = 0.0005$ otherwise.

Regression Analysis of Measured Spectra. To analytically represent measured spectra $S(\nu_n)$ by relaxation spectral functions $R(\nu_n, P_j)$ we used a Marquardt algorithm[18] to minimize the variance

$$\chi^2(P_1, ..., P_J) = \frac{1}{N - J - 1}\sum_{n=1}^{N}\left(\frac{S(\nu_n) - R(\nu_n, P_j)}{\Delta S(\nu_n)}\right)^2 \qquad (4)$$

Here ν_n, $n = 1, ..., N$, are the frequencies of measurement, P_j, $j = 1, ..., J$, are the parameters of R, and $\Delta S(\nu_n)$ denotes the experimental error of S at ν_n. ΔS^{-1} is used as weighing factor in eq 4.

3. Results and Analytical Description of Spectra

Sonic Absorption Spectra. In Figure 1 the frequency-normalized ultrasonic absorption spectrum of pentadecane is displayed at 15 °C. If relaxation processes are missing in acoustical spectra, frequency-independent η_s and η_v result in a constant α/ν^2 (eq 1). The α/ν^2 data for *n*-pentadecane, however,

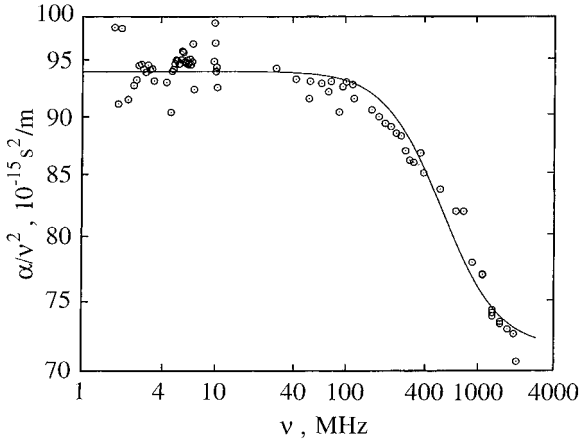

Figure 1. Ultrasonic absorption coefficient per ν^2 for *n*-pentadecane at 25 °C plotted versus frequency ν. The curve represents a relaxation function with discrete relaxation time.

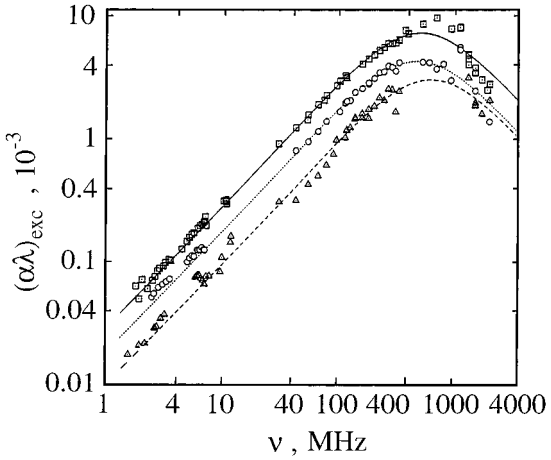

Figure 2. Ultrasonic absorption spectra in the format $(\alpha\lambda)_{ex}$ vs ν for *n*-pentadecane/*n*-hexane mixtures at different mole fraction x of *n*-pentadecane. □, $x = 1$; ○, $x = 0.75$; △, $x = 0.5$; 15 °C. The full, dashed, and dotted lines are graphs of the $R_\alpha(\nu)$ function (eq 8) with the parameters given in Table 2.

at $\nu > 100$ MHz clearly decrease with frequency, thus indicating relaxation behavior. Because the relaxation frequency obviously is high, it is useful to plot the data also in the format $(\alpha\lambda)_{exc}$ vs ν, in which the high-frequency part of the spectrum is accentuated. Here $\lambda = c/\nu$ is the sonic wavelength and suffix exc indicates that only the part of the total absorption per wavelength, $\alpha\lambda$, that exceeds the high-frequency asymptotic background contribution, $(\alpha\lambda)_{asy}$, is shown

$$(\alpha\lambda)_{exc} = (\alpha\lambda) - (\alpha\lambda)_{asy} \tag{5}$$

In plotting the $(\alpha\lambda)_{exc}$ spectra

$$(\alpha\lambda)_{asy} = B\nu \tag{6}$$

has been assumed with B independent of ν, corresponding with a constant part $B' = Bc$ in the frequency-normalized spectrum (Figure 1). The $(\alpha\lambda)_{exc}$ spectra displayed in Figure 2 confirm the relaxation characteristics in the sonic absorption of *n*-pentadecane. These spectra also show that the amplitude of the excess absorption becomes smaller when *n*-hexane is added to *n*-pentadecane whereas the relaxation frequency $\hat{\nu}$ is almost independent of the mixture composition. Here $\hat{\nu}$ is simply defined as the frequency at which the $(\alpha\lambda)_{exc}$ vs ν relation adopts its maximum. These dilution properties suggest an underlying unimolecular reaction of the type[19]

$$A \underset{k_b}{\overset{k_f}{\rightleftharpoons}} A^* \tag{7}$$

Closer inspection of the spectra leads to the conclusion that, within the limits of experimental error, all but one can be well represented by a relaxation term with discrete relaxation time τ_α. Hence we used the relaxation spectral function

$$R_\alpha(\nu) = A_\alpha \frac{\omega\tau_\alpha}{1 + (\omega\tau_\alpha)^2} + B\nu \tag{8}$$

to represent the frequency-dependent $\alpha\lambda$ data. Herein A_α is the relaxation amplitude. In deriving eq 8 it has been tacitly taken into account that the dispersion in the sound velocity is small. Hence $c(\nu)/c(\nu \rightarrow \infty) = 1$ has been used. The A_α, τ_α, and B values following from the nonlinear least-squares regression analysis of the measured spectra are collected in Table 2 where the sound velocities are also given.

The only sample of which the spectrum cannot be adequately represented by the $R_\alpha(\nu)$ function (eq 8) is the *n*-eicosane/*n*-tetradecane mixture. As illustrated by Figure 3 the excess absorption region for this liquid extends over a somewhat broader frequency range than predicted by eq 8. We suppose this broadening to be due to a superposition of two relaxation terms, assuming both constituents of the mixture to display their own ultrasonic relaxation. For simplicity we assumed these relaxation mechanisms to proceed independently from another. We therefore analyzed the *n*-eicosane/*n*-tetradecane spectrum in terms of two relaxation contributions with discrete relaxation time. In doing so we fixed the relaxation time τ_α^* of one of the terms at the value for *n*-tetradecane at the same temperature ($\tau_\alpha^* = 0.19$ ns, 25 °C, Table 2). The fitting procedure yielded a relaxation amplitude $A_\alpha^* = 0.014 \pm 0.003$, in agreement with our expectations due to simple mixture relations ($A_\alpha^* = 0.012 \pm 0.002$). It seems thus to be justified to consider τ_α and A_α the parameters of the *n*-eicosane relaxation process.

Shear Viscosity Relaxation. In Figure 4, as an example, the real part η_s' and the negative imaginary part η_s'' of the complex shear viscosity of *n*-hexadecane, as following from the shear impedance measurements (eq 3), are displayed as a function of frequency ν. Within the frequency range of measurement η_s' decreases slightly from $\eta_s' = (3.1 \pm 0.1) \times 10^{-3}$ Pa·s at 20 MHz to $\eta_s' = (2.9 \pm 0.3) \times 10^{-3}$ Pa·s at 120 MHz. With all studied alkanes the small frequency dependence in the real part of the viscosity does not exceed the experimental uncertainty. However, corresponding with the decrease in $\eta_s'(\nu)$, the negative imaginary part η_s'' increases almost proportional to ν. This behavior is characteristic for the low-frequency wing of a relaxation process. Hence we analyzed the shear viscosity spectra in terms of the relaxation spectral function ($i^2 = -1$)

$$R_s(\nu) = \eta_s(\infty) + \frac{A_s}{1 + i\omega\tau_s} \tag{9}$$

Since the frequency range of the shear viscosity measurements is too small to allow for a reliable determination of the three parameters $\nu_s(\infty)$, A_s, and τ_s of the $R_s(\nu)$ function, we assumed both the ultrasonic relaxation and the shear viscosity relaxation to be due to the same molecular mechanism. Hence we used

$$\tau_s = \tau_\alpha \tag{10}$$

in the evaluation of the measured spectra. The results for the

TABLE 2: Sound Velocity *c* and Parameters of the Ultrasonic Spectrum (Eq 8) for *n*-Alkanes at the Temperature *T*[a]

sample	*T*, °C	*c*, m/s	A_α, 10^3	τ_α, ps	*B*, ps
n-tetradecane	10.0(2)	1368(6)	18(2)	240(20)	91(1)
	18.5(1)	1336(6)	16(2)	220(30)	84(1)
	25.0(1)	1313(6)	16.9(15)	190(10)	78.6(7)
n-pentadecane	25.0(1)	1324(6)	15.0(15)	250(20)	86.6(9)
	20.0(1)	1345(6)	14.5(13)	270(20)	91.7(10)
	15.0(2)	1364(6)	14.4(9)	320(10)	98(1)
n-pentadecane/*n*-hexane ($x = 0.75$)	15.0(1)	1332(6)	9.05(33)	324(21)	84(1)
n-pentadecane/*n*-hexane ($x = 0.5$)	15.0(1)	1295(6)	5.5(13)	287(50)	72(1)
n-hexadecane	18.5(2)	1363(6)	14.4(5)	390(10)	101.8(6)
	20.0(1)	1359(6)	16.0(10)	330(10)	98.0(10)
	25.0(1)	1336(6)	16.8(7)	290(10)	91.9(5)
n-eicosane/*n*-tetradecane ($x = 0.333$)	25.0(1)	1333(6)	5.3(15)	520(70)	92.0(8)

[a] With the *n*-eicosane/*n*-tetradecane mixture parameters A_α and τ_α refer to the eicosane relaxation. A second relaxation term has been found in the spectrum ($A_\alpha^* = 0.0014$, $\tau_\alpha^* = 0.19$ ns) and has been attributed to *n*-tetradecane.

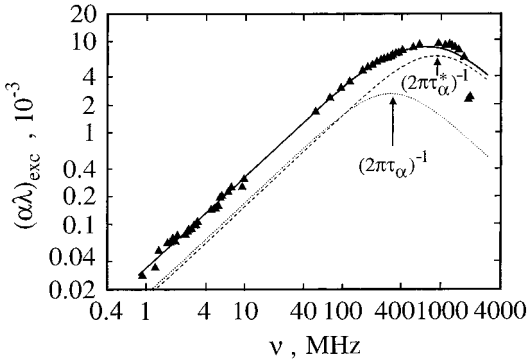

Figure 3. Ultrasonic excess absorption spectrum of the *n*-eicosane/*n*-tetradecane mixture at 25 °C. Dashed and dotted curves show the subdivision of the spectrum into two relaxation terms with relaxation times τ_α^* and τ_α, respectively. The full curve represents the superposition of both terms.

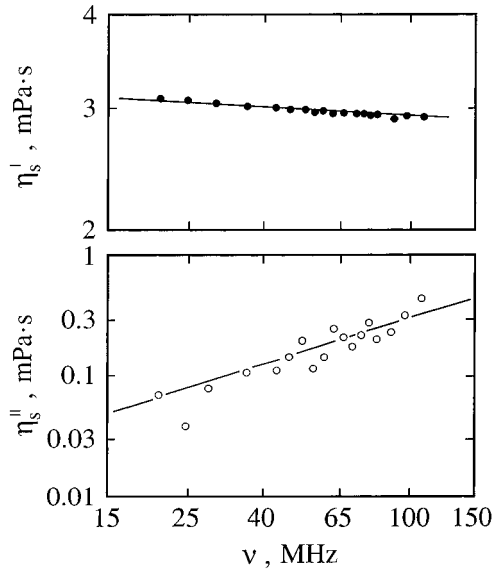

Figure 4. Real part η_s' (●) and negative imaginary part η_s'' (○) of the complex shear viscosity of *n*-hexadecane at 25 °C displayed as a function of frequency. The curve is a graph of the Debye-type spectral function defined by eq 9 with the parameter values given in Table 3.

high-frequency viscosity $\eta_s(\infty)$, the relaxation amplitude A_s, and the static viscosity

$$\eta_s(0) = \eta_s(\infty) + A_s \tag{11}$$

are given in Table 3. It is found that the $\eta_s(0)$ data from the high-frequency measurements within the limits of experimental error agree with the static values η_{s0} as determined with the normal viscometers. This agreement may be taken to indicate the absence of systematic errors in the shear wave impedance spectrometry.

4. Discussion

Conformational Modes and Orientational Motions. As illustrated by Figure 5 the τ_α data of the *n*-alkanes depend strongly upon the length of the molecules. Furthermore the ultrasonic relaxation times for *n*-dodecane, *n*-tetradecane, and *n*-hexadecane agree almost perfectly with molecular reorientation times as derived from depolarized Rayleigh scattering.[20] Both findings indicate a structural relaxation process in which motions of the complete molecules are involved. On the other hand, dielectric relaxation times τ_d are substantially smaller than τ_α (Figure 5), for example, $\tau_d(20\ °C)/\tau_\alpha(25\ °C) = 0.07$ for *n*-dodecane. The τ_d values have been taken from microwave and far-infrared spectra of a series of *n*-alkanes.[21,23] Here the τ_d values are just defined by the frequency ν_d ($=(2\pi\tau_d)^{-1}$) at which the microwave dielectric loss data adopt a relative maximum.[22] A careful analysis shows[23] that, in the 5−500 GHz range, the dielectric spectra of the *n*-alkanes are subject to a Fröhlich relaxation time distribution (Figure 6) involving a minimum and a maximum relaxation time.[24] The more sophisticated evaluation of the measured dielectric spectra in terms of a continuous relaxation time distribution function, however, is of low significance for the present discussion.

The dielectric relaxation of the nondipolar *n*-alkanes is considered to be due to temporary collision-induced moments at the molecule ends.[23] Within the framework of that model the relaxation time τ_d is the mean lifetime of the induced moments, and it has been reasoned that this lifetime is mainly determined by the translational motions of the alkane molecules.[23] As might be suggested intuitively, with long-chain *n*-alkanes rotational molecular motions around short axes of inertia are much more hindered than translational motions in the direction of the major molecular axis. The latter will thus predominate.[25] Following these lines of reasoning the finding of the orientation correlation times τ_{or} to substantially exceed the dieletric relaxation times τ_d reflecting translational motions is a reasonable result. The strong correlation between the τ_{or} data and the ultrasonic relaxation times τ_α (Figure 5), which are obviously given by the relaxation rates

$$1/\tau_\alpha = k_f + k_r \tag{12}$$

of unimolecular reactions (eq 7), suggests the reorientation of an *n*-alkane molecule to be coupled to a conformational relaxation process. This coupling may be illustrated as follows.

TABLE 3: Fitted High-Frequency Viscosity $\eta_s(\infty)$, Relaxation Amplitude A_s, and Relaxation Time τ_s (Eq 9), as Well as the Fitted Low-Frequency Viscosity $\eta_s(0)$ (Eq 11) for Some *n*-Alkane Systems at 25 °C

sample	$\eta_s(\infty)$, mPa·s ±10%	A_s, mPa·s ±20%	τ_s, ns ±10%	$\eta_s(0)$, mPa·s ±10%
n-tetradecane				2.06
n-pentadecane	1.27	1.19	0.25	2.46
n-hexadecane	1.23	1.74	0.29	2.97
n-eicosane/*n*-tetradecane, $x = 0.333$	1.89	1.19	0.52	3.08

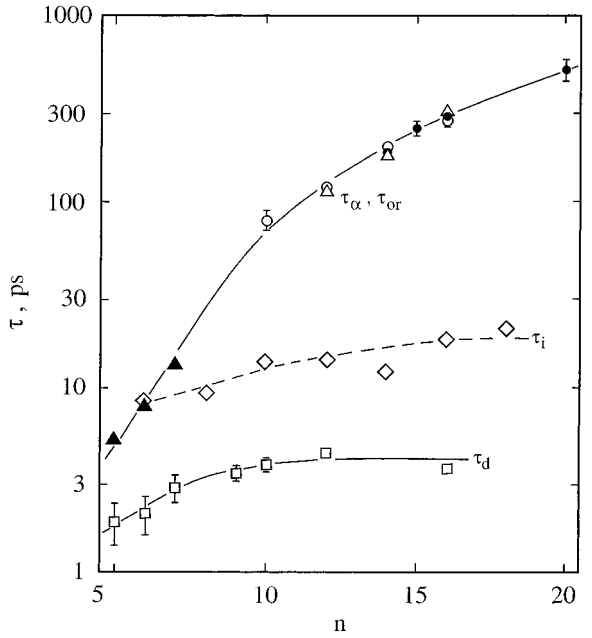

Figure 5. Relaxation times at 25 and 20 °C from ultrasonic spectroscopy (τ_α; ○, ref 4; ●, this paper), depolarized Rayleigh scattering (τ_{or}; △, ref 25; ▲, ref 20), ^{13}C NMR (τ_i; ◇, ref 26), and dielectric spectroscopy (τ_d; □, ref 23) plotted versus the number *n* of carbon atoms per *n*-alkane molecule C_nH_{2n+2}.

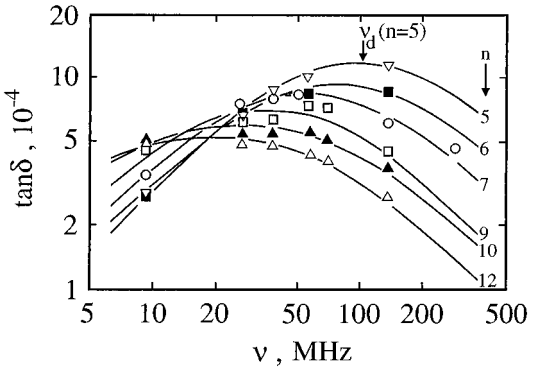

Figure 6. Microwave part of the dielectric loss factor spectrum for a series of *n*-alkanes at 20 °C.[23] The loss factor is defined by $\tan\delta = \epsilon''(\nu)/\epsilon'(\nu)$, where ϵ'' and ϵ' are the negative imaginary part and the real part, respectively, of the complex (electric) permittivity.

During a period τ_α an alkane molecule is subject to a large number of thermally driven collisions with neighboring molecules. The high flexibility will result in changes of the molecular conformation. Rotation around an individual C−C bond occurs rather often, as indicated by the τ_i data in Figure 5 ($\tau_i/\tau_d \approx 2$ for *n*-dodecane). Rotational isomerization of the long-chain normal alkanes as reflected by the ultrasonic relaxation process, however, cannot considered a sum of independent individual bond rotations as observed with the smaller homologues. Rather it constitutes a collective phenomenon depending on the length of the alkanes.[2] Hence for the higher homologues τ_α is significantly greater than the individual C−C bond correlation time τ_i as derived from nuclear magnetic ^{13}C relaxation times,[26] $\tau_\alpha/\tau_i \approx 9$ for *n*-dodecane (Figure 5). The similarity of τ_{or} and τ_α data in Figure 5 reveals reorientation of an *n*-alkane through a significant angle around the short axis of inertia to occur with the frequency of conformational changes. Hence $\tau_{or} \approx \tau_\alpha$ suggests the reorientation time to mainly reflect the time for which a molecule has to wait until a conformational transition results in favorable conditions for the orientational motion. This view involves the reorientation itself to follow a jump mechanism.

Reaction Volume. Number of Cis−Trans Configurations. These ideas of molecular motions in long-chain liquid *n*-alkanes are based just upon the relative order of magnitude in the relaxation times of different parameters of the liquid. We now attempt to verify the above view of conformational isomerizations to play a central role in the microdynamics of *n*-alkanes by detailed evaluation of the measured relaxation spectra.

Assuming a unimolecular reaction (eq 7), the amplitude A_α of the ultrasonic relaxation term (eq 8) according[1,19]

$$A_\alpha = \frac{\pi\Gamma c_\infty^2 \rho}{RT}\left(\frac{A_\infty}{\rho c_{p\infty}}\Delta H + \Delta V\right)^2 \qquad (13)$$

is given by the reaction volume ΔV, the reaction enthalpy ΔH, and the stoichiometric factor Γ, defined by

$$\Gamma^{-1} = [\mathrm{A}]^{-1} + [\mathrm{A}^*]^{-1} \qquad (14)$$

In eq 13 the heat capacity at constant pressure and the thermal expansion coefficient for frequencies well above the relaxation frequency ($\nu \gg (2\pi\tau_\alpha)^{-1}$) are given by[1,19]

$$c_{p\infty} = c_{p0} - \frac{\Gamma(\Delta H)^2}{\rho RT^2} \qquad (15)$$

and

$$A_\infty = \lim_{\omega\to 0}\left[\frac{1}{V}\left(\frac{\partial V}{\partial T}\right)_p\right] - \frac{\Gamma\Delta H\Delta V}{RT} \qquad (16)$$

respectively.

Let us consider eqs 13 and 14 in light of the model of coupled hypothetical torsional oscillators,[2,27,28] as originally derived to describe the modes of polymer chain motions.[29,30] The coupled torsional oscillator model yields a series of relaxation terms. We assume the ultrasonic absorption spectra of alkanes to reflect the relaxation mode with the lowest relaxation frequency, representing the transition from an all-trans configuration of the chain molecule to a configuration in which the mean number *k* of rotated C−C bonds per alkane molecule is adopted. If ΔV_o denotes the molar volume change associated with the rotation of a single C−C bond

$$\Delta V = k\Delta V_o \qquad (17)$$

where $\Delta V = 1.8$ cm^3/mol, as following from the volume change of long-chain *n*-alkanes.[31] Let $c_{mol} = [C_nH_{2n+2}]$ denote the molar concentration of the *n*-alkanes. The concentration of cis−trans and trans−trans configurations is then given by $[\mathrm{A}^*] = kc_{mol}/$

TABLE 4: Gibbs Free Activation Energy $\Delta G^{\ddagger}$ Resulting from the Relaxation Times (Eq 19) on Alternative Assumptions upon the Number n_{to} of Individual Oscillators per Alkane Molecule, as Well as the Activation Enthalpy $\Delta H^{\ddagger}$ and Entropy $\Delta S^{\ddagger}$ Following from Temperature-Dependent Measurements (Eq 20)[a]

	$n_{to} = n$	$n_{to} = n/2$	$n_{to} = n/3$		
alkane	$\Delta G^{\ddagger}$, kJ/mol	$\Delta G^{\ddagger}$, kJ/mol	$\Delta G^{\ddagger}$, kJ/mol	$\Delta H^{\ddagger}$, kJ/mol	$\Delta S^{\ddagger}$, J/mol, K
n-decane[4]	7.3	10.9	12.8		
n-dodecane[4]	8.8	12.2	14.1		
n-tetradecane	9.2	12.6	14.5	16.4	6
n-pentadecane	9.5	12.9	14.9	18.2	11
n-hexadecane	9.5	13.0	15.0	19.1	13
n-eicosane	9.9	13.3	15.3		

[a] All data refer to 25 °C.

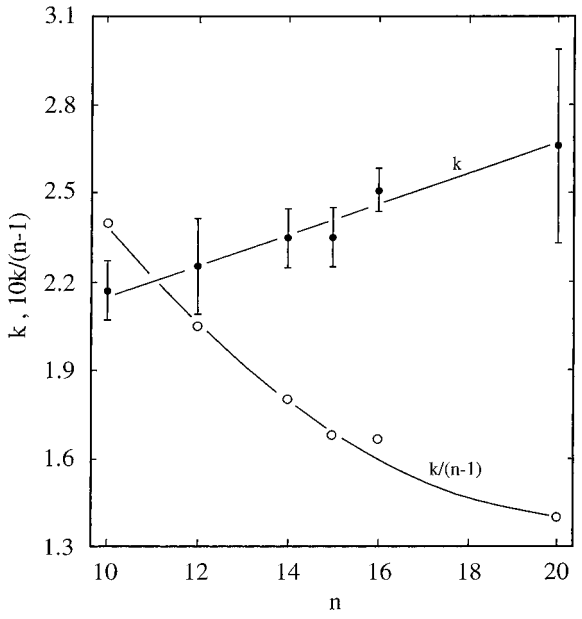

Figure 7. Mean number k of rotated C−C bonds per alkane molecule and fraction $k/(n-1)$ of rotated bonds as a function of the number n of carbon atoms per *n*-alkane molecule.

$(n-1)$ and $[A] = (1-k)c_{mol}/(n-1)$, respectively, so that

$$\Gamma = \frac{k}{n-1}\left(1 - \frac{k}{n-1}\right) \tag{18}$$

Use of reasonable reaction enthalpies ΔH[20] results in contributions of the enthalpy term to the relaxation amplitude A_α (eq 13) that do not exceed the experimental error ΔA_α. We therefore neglected the effect from the enthalpy term to calculate k, using eqs 17 and 18 together with relation 13. The results of this calculation are shown in Figure 7. The mean number of rotated C−C bonds per alkane molecule increases from $k = 2.2$ with *n*-decane to $k = 2.7$ with *n*-eicosane. Since the k-value derived from the relaxation amplitude depends on the ΔV_o value used in eq 17 and because this value is not precisely known, the absolute number of cis−trans configurations should not be overemphasized. Nevertheless a tendency is found in the relative content of rotated C−C bonds to decrease with chain length: $k/(n-1) = 0.24$ at $n = 10$ and $k/(n-1) = 0.14$ at $n = 20$. According to eq 17 the slightly increasing k-values displayed in Figure 7 result in a reaction volume that also increases with the length of *n*-alkane molecule, from $\Delta V = 3.9$ cm^3/mol for *n*-decane to $\Delta V = 4.8$ cm^3/mol for *n*-eicosane.

Number of Coupled Oscillators. Free Energy of Activation. Originally, in the model of coupled torsional oscillators allowance was made for two or three carbon atoms in the alkyl chain to move as one oscillating unit.[27,28] The number n_{to} of individual oscillators per alkane C_nH_{2n+2} was thus assumed to equal either $n/2$ or $n/3$. Later $n_{to} = n$ has been preferred.[2]

The first normal mode of the coupled system of torsional oscillators corresponds to the relaxation term with the smallest relaxation frequency. Hence the relaxation time τ_1 of that mode is identified with the relaxation time τ_α in the ultrasonic spectra. It is given by the relation[27,28]

$$\tau_1^{-1} = 2\nu_{to} \sin^2\left(\frac{\pi}{2n_{to}}\right) e^{-\Delta G^{\ddagger}/RT} \tag{19}$$

with the characteristic frequency ν_{to} for the rotation of a single C−C bond and with the Gibbs free energy of activation

$$\Delta G^{\ddagger} = \Delta H^{\ddagger} - T\Delta S^{\ddagger} \tag{20}$$

where $\Delta H^{\ddagger}$ and $\Delta S^{\ddagger}$ denote the enthalpy and entropy of activation, respectively. Assuming ν_{to} to be independent of the length of *n*-alkane molecules, we used $\nu_{to} = 8.5$ THz as reported for ethane.[32] The $\Delta G^{\ddagger}$ values following for the alternative n_{to} values are presented in Table 4. If these values are compared to the experimental activation energies $\Delta G^{\ddagger} = 14.2$ kJ/mol for *n*-propane[32] and $\Delta G^{\ddagger} = 14.5$ kJ/mol for *n*-butane,[32] the assumption of $n_{to} = n/3$ appears to be most realistic. This statement contradicts the results by Cochran et al. who preferred $n_{to} = n$.[2] However, those authors considered the $\Delta G^{\ddagger}$ values from eq 19 in light of $\Delta G^{\ddagger} = 12.1$ kJ/mol for ethane. We suppose that ethane, with its one C−C bond only, constitutes a special case and that comparison to the activation energies of higher homologues is more appropriate.

Since we measured some *n*-alkanes at different temperatures, we used eq 20 to calculate the activation enthalpy and entropy for these liquids, assuming $\Delta H^{\ddagger}$ and $\Delta S^{\ddagger}$ to be independent of T in the limited measuring range. As expected intuitively, $\Delta H^{\ddagger}$ and $\Delta S^{\ddagger}$ seem to increase with chain length n (Table 4).

Isomerization−Viscosity Coupling. Shear Viscosity Dispersion Amplitude. According to the model of coupled damped torsional oscillators,[2,27,28] an *n*-alkane molecule is capable of the large number $3^{n_{to}}$ of different conformations of which the all-trans conformation is the most stable one. The liquid may respond to a shear gradient by two molecular mechanisms, reorientation of complete molecules as rigid rod-shaped units or deformation of the molecules by intramolecular structural isomerization. Both modes of molecular motions tend to facilitate mutual movements of neighboring molecular layers and thus act an influence on the viscoelastic properties of the liquid. For this reason, Tobolsky, when presenting the model of coupled damped torsional oscillators,[27] predicted a shear viscosity relaxation.

As already indicated when discussing the different relaxation times of *n*-alkanes (Figure 5), reorientation of a molecule without a significant change of its conformation during the

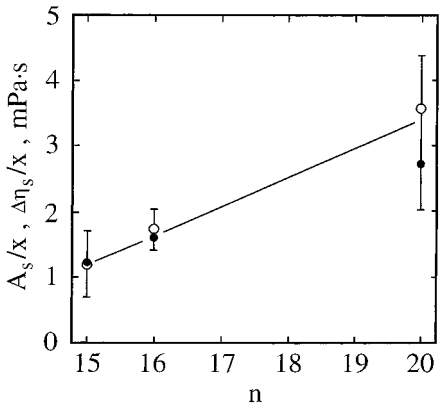

Figure 8. Relaxation amplitude A_s derived from the shear viscosity spectra (○, eq 9) and shear viscosity step $\Delta\eta_s$ resulting from the ultrasonic spectra (●, eq 21), normalized to the mole fraction x of n-alkane under consideration, at 25 °C, displayed versus the number n of carbon atoms per alkane molecule C_nH_{2n+2}.

orientation time τ_{or} is unlikely. Rather the reorientation appears to be stimulated by rotational isomerization. If this is accepted a viscosity relaxation with discrete relaxation time τ_s and also the conformity of relaxation times $\tau_s = \tau_\alpha = \tau_{or}$ appears to be a plausible assumption. If the observed frequency dependence in the complex shear viscosity (Figure 4) is due to the rotational isomerization of *n*-alkane molecules, as described by the coupled torsional oscillator model, then the observed relaxation strength $A_s = \eta_s(0) - \eta_s(\infty)$ (Table 3) must agree with the predictions from the ultrasonic relaxation term. If the latter (eq 8) is assumed to reflect a shear viscosity relaxation with relaxation amplitude $\Delta\eta_s$, eq 1 yields

$$\Delta\eta_s = \frac{3}{4\pi}\rho c_s^2 A_\alpha \tau_\alpha \qquad (21)$$

In Figure 8 the $\Delta\eta_s$ values from the ultrasonic relaxation parameters (eq 21) are compared to the A_s data directly obtained from shear wave impedance spectrometry. The agreement between both sets of data confirms the idea of cooperative structural isomerizations to stimulate reorientational motions and to be accompanied by a high-frequency viscosity relaxation. Sceats and Dawes[3] have doubted this idea because the ultrasonic relaxation times by Cochran et al.[2] do not agree with the orientational correlation times τ_{or} from depolarized Rayleigh scattering studies. It turns out that this discrepancy was just due to the limited accuracy of those ultrasonic relaxation data but that the scenario of molecular motions developed by Tobolsky[27] and Cochran et al.[2] is in conformity with our present ultrasonic and shear viscosity relaxation spectra.

References and Notes

(1) Litovitz, T. A.; Davis, C. M. In *Physical Acoustics, Principles and Methods*; Mason, W. P., Ed.; Academic Press: New York, 1965; Vol. 2, Part A.
(2) Cochran, M. A.; Jones, P. B.; North, A. M.; Pethrick, R. A. *J. Chem. Soc., Faraday Trans. 2* **1972**, *68*, 1719.
(3) Sceats, M. G.; Dawes, J. M. *J. Chem. Phys.* **1985**, *83*, 1298.
(4) Kaatze, U.; Lautscham, K.; Berger, W. *Chem. Phys. Lett.* **1988**, *144*, 273.
(5) Herzfeld, K. F.; Litovitz, T. A. *Absorption and Dispersion of Ultrasonic Waves*; Academic Press: New York, 1959.
(6) Madigosky, W. M.; Warfield, R. W. *Acustica* **1984**, *55*, 123.
(7) Eggers, F.; Kaatze, U.; Richmann, K. H.; Telgmann, T. *Meas. Sci. Technol.* **1994**, *5*, 1131.
(8) Kaatze, U.; Wehrmann, B.; Pottel, R. *J. Phys. E: Sci. Instrum.* **1987**, *20*, 1025.
(9) Kaatze, U.; Lautscham, K.; Brai, M. *J. Phys. E: Sci. Instrum.* **1988**, *21*, 98.
(10) Bömmel, H. E.; Dransfeld, K. *Phys. Rev. Lett.* **1958**, *1*, 234.
(11) Kaatze, U.; Lautscham, K. *J. Phys. E.: Sci. Instrum.* **1988**, *21*, 402.
(12) Kaatze, U.; Kühnel, V.; Weiss, G. *Ultrasonics* **1996**, *34*, 51.
(13) Behrends, R.; Kaatze, U. Submitted for publication in *Meas. Sci. Technol.*
(14) Eggers, F.; Funck, T. *J. Phys. E.: Sci. Instrum.* **1987**, *20*, 523.
(15) Nowotny, H.; Benes, E. *J. Acoust. Soc. Am.* **1987**, *82*, 513.
(16) Reed, C. E.; Kanazawa, K. K.; Kaufmann, J. H. *J. Appl. Phys.* **1990**, *68*, 1993.
(17) Eggers, F.; Kaatze, U. *Meas. Sci. Technol.* **1996**, *7*, 1.
(18) Marquardt, D. W. *J. Soc. Indust. Appl. Math.* **1963**, *2*, 2.
(19) Strehlow, H.; Knoche, W. *Rapid Reactions in Solutions*; VHC−Verlagsgesellschaft: Weinheim, 1992.
(20) Champion, J. V.; Jackson, D. A. In *Molecular Motions in Liquids*; Lascombe, J., Ed.; Reidel: Dordrecht, 1974.
(21) Göttmann, O.; Stumper, U. *Chem. Phys. Lett.* **1973**, *22*, 387.
(22) Stumper, U. In *Molecular Motions in Liquids*; Lascombe, J., Ed.; Reidel: Dordrecht, 1974.
(23) Stumper, U. *Adv. Mol. Relaxation Proc.* **1975**, *7*, 189.
(24) Fröhlich, H. *Theory of Dieletrics*, 2nd ed.; Oxford University Press: London, 1958.
(25) Volterra, V.; Bucaro, J. A.; Litovitz, T. A. *Ber. Bunsen-Ges. Phys. Chem.* **1971**, *75*, 309.
(26) Levine, Y. K.; Birdsall, N. J. M.; Lee, A. G.; Metcalfe, J. C.; Partington, P.; Roberts, G. C. K. *J. Chem. Phys.* **1974**, *60*, 2890.
(27) Tobolsky, A. V. *J. Polym. Sci. A-2*, **1968**, *6*, 1177.
(28) Tobolsky, A. V.; DuPré, D. B. *Adv. Polym. Sci.* **1969**, *6*, 103.
(29) Rouse, P. E. *J. Chem. Phys.* **1943**, *21*, 1272.
(30) Zimm, B. H. *J. Chem. Phys.* **1956**, *24*, 269.
(31) Träuble, H.; Haynes, D. *Chem. Phys. Lipids* **1971**, *7*, 324.
(32) Pitzer, K. S. *J. Chem. Phys.* **1944**, *12*, 310.